IFAI Geosynthetics Conference
Feb. 10-13, 2019 | Houston, TX USA

Wave-Induced Instability of Seabed Beneath Geotextile Sand Containers

Amin Rafiei, Graduate Research Assistant,[1] M.A. Gabr, Professor,[2] and M.S. Rahman[3], Professor

[1]North Carolina State University, Department of Civil, Construction and Environmental Engineering, Raleigh, NC, USA 27607; e-mail: arafiei@ncsu.edu
[2]North Carolina State University, Department of Civil, Construction and Environmental Engineering, NC, USA 27607; e-mail: rahman@ncsu.edu
[3]North Carolina State University, Department of Civil, Construction and Environmental Engineering, Raleigh, NC, USA 27607; e-mail: gabr@ncsu.com

ABSTRACT

The use of geotextile tubes for shoreline protection has widely spread. In many cases, geotextile containers consist of geotextile layers that are filled hydraulically with dredge soil. The failure of these structures (as coastal protective systems) during storm events has been reported, as for example during Hurricane Ike. While numerous studies have investigated the internal stability of geotextile container, few are done on the stability due to wave action. The applied wave loading on geotextile containers are mostly obtained from simplified analytical solutions. In this paper, the external stability of geotextile container is studied with a focus on instability of the foundation soil (seabed) due to wave-induced instantaneous liquefaction. The characteristics of liquefaction around the structure is investigated through a parametric study. In addition, the loading distribution acting on the structure is evaluated. The foundation soil is represented by a poroelastic domain, and the full coupling between domains (wave, geotextile container, and seabed) is considered. The results show the development of liquefied zone around the geotextile container leading to instability of the structure under wave loading.

INTRODUCTION

The protection of shorelines from storm waves and sediment erosion is a significant challenge in coastal engineering. Among various coastal structures such as breakwaters and seawalls, geotextile sand containers (GSCs) have attracted attentions recently as they potentially offer an environmentally friendly cost-effective solution (Recio 2008). GSCs are comprised of a geotextile bag filled with a mixture of soil and water. Although GSCs are desirable beach protection system, numerous failure cases caused by wave action have been reported given the complexity of the loading scheme due to wave action and lack of knowledge in design procedures (Heilman et al. 2008, Kraus et al. 2009, Khalilzad and Gabr. 2011).

The instability of GSCs is classified into internal and external failure mechanisms (Neves 2011). The internal failure is mostly related to the tearing of geotextile, loss of the strength of fill material (due to increase in excess pore fluid pressure and consequent liquefaction) and internal movement of the confined soil. The external instability refers to sliding and overturning of the structure, loss of bearing capacity of foundation soil, and scour around the GSCs. Recio (2008) in

an experimental and numerical study examined the effects of deformation of GSC-structures on their hydraulic stability and concluded that deformation reduces contact areas and resisting forces between the containers resulting in instability of the structure. Neves (2011) studied the wave-induced scour due to sediment transport near the geotextile encapsulated-sand systems. Based on laboratory measurements, Neves demonstrated that the maximum scour depth decreases with an increase in the water depth at the structure, and the scour depth is larger when waves are breaking near the toe of the structure (Neves 2011).

Among recent studies in stability analysis of GSCs, there are only a few studies focusing on instability of foundation soil near the structure. The surface waves in shallower water (common deployment locations of GSCs) induces a significant amount of pore fluid pressure inside the seabed causing the reduction of effective stress in sediments. This, in turn, will decrease the shear strength of sediments and cause liquefaction in severe cases. Liquefaction-induced scour due to instability of seabed has been identified to be a major threat to coastal structures (Robertson et al. 2009).

In this paper, the wave-induced response and instability of seabed near the GSC with a focus on instantaneous liquefaction is studied. The full interactive process between media (fluid, GSC, and seabed) is included in the analysis; however, the effect of presence of the structure on the wave profile change is not considered herein. The deployment location of a single submerged GSC is assumed to be prior to wave breaking zone in shallow water where linear wave theory is applicable. Biot's poro-elastic theory for the sediment, u-p approximation (Biot 1956), linear waves and potential flow for the fluid (Dean and Dalrymple 1984), and elastodynamic equations (Bathe 1996) for the structure domains are solved simultaneously in a coupled finite element model. The distribution of wave loading acting on the structure as well as the extent of liquefied zone are presented.

GOVERNING EQUATIONS

The equations governing each domain, fluid, geotextile, confined soil, and seabed are presented herein. The analyses are carried out for two-dimensional plane strain condition. The general sketch of the reference problem for a single submerged GSC is indicated in Figure 1.

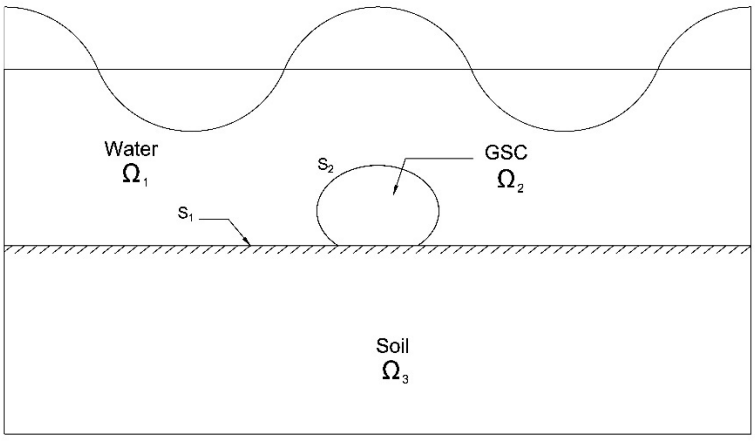

Figure 1. Schematic sketch of the reference problem

Fluid Domain. GSCs may be installed in different locations. While, some of the GSCs are mounted near the beach line in which a portion of the structure may be above the mean water level, some are completely submerged but are still in shallow water (e.g. submerged sill). In shallow water various wave theories are applicable depending on wave characteristics (Dean and Dalrymple 1984). In this study, it is assumed that the GSC is submerged and placed in shallow water prior to wave breaking zone. Also, the fluid is assumed to be inviscid and incompressible with irrotational flow; thus, linear wave theory is employed for modeling the waves. Although in storm condition, a more realistic wave loading is obtained based on nonlinear waves, linear waves are adopted as the first approximation in this work. The governing equation is expressed as:

$$\nabla^2 \emptyset = 0 \tag{1}$$

where $\emptyset$ denotes velocity potential. The velocity (v_f) and hydrodynamic pressure (p_f) corresponding to velocity potential are written as:

$$v_f = -\nabla \emptyset \tag{2}$$

$$p_f = \rho_f \dot{\emptyset} \tag{3}$$

in which ρ_f denotes water density.

GSCs Domain. The permeability of geotextile is normally within the range of sand fill (Mirafi 2004). In this study, however, since the external stability of the structure with respect to liquefaction in seabed is considered, the hydraulic properties of geotextile and confined soil are neglected, and the structure is assumed as elastic body defined by the following elastodynamic equations in plane strain condition:

$$G_{st}\nabla^2 u_{st} + \frac{G_{st}}{1-2\vartheta}\frac{\partial \varepsilon_{v,st}}{\partial x} + F_{B,x} = \rho_{st}\frac{\partial^2 u_{st}}{\partial t^2} \tag{4}$$

$$G_{st}\nabla^2 v_{st} + \frac{G_{st}}{1-2\vartheta}\frac{\partial \varepsilon_{v,st}}{\partial z} + F_{B,y} = \rho_{st}\frac{\partial^2 v_{st}}{\partial t^2} \tag{5}$$

in which G_{st}, ϑ, and ρ_{st} are shear modulus, Poisson's ratio, and density of the structure domain, respectively, u_{st}, v_{st} are displacement components, $\varepsilon_{v,st}$ is volumetric strain of the structure element, and F_B denotes the body force vector per unit volume. It is common to assume GSCs as impermeable media for the purpose of conducting external stability analyses (e.g. Khalilzad and Gabr 2011).

Seabed Domain. The sediments are defined by Biot's poroelasticity theory in partly dynamic form, u-p approximation (Biot 1956). The acceleration of pore water is neglected in this formulation and it is assumed that the pore fluid flow obeys Darcy's law. For a homogenous isotropic medium the equations in plane strain condition take the form as:

$$G\nabla^2 u + \frac{G}{1-2\vartheta}\frac{\partial \varepsilon_v}{\partial x} = \frac{\partial p}{\partial x} + \rho\frac{\partial^2 u}{\partial t^2} \tag{6}$$

$$G\nabla^2 v + \frac{G}{1-2\vartheta}\frac{\partial \varepsilon_v}{\partial z} = \frac{\partial p}{\partial z} + \rho\frac{\partial^2 v}{\partial t^2} \tag{7}$$

$$k\nabla^2 p - \gamma_w n\,\beta\,\dot{p} + k\,\rho_f\frac{\partial^2 \varepsilon_v}{\partial t^2} = \gamma_w\frac{\partial \varepsilon_v}{\partial t} \tag{8}$$

where p is pore water pressure, and u and v are the soil skeleton displacements in horizontal and vertical directions, respectively, G shear modulus, ε_v volumetric strain of the soil element, γ_w water unit weight, k and n permeability and porosity of sediment. The total density of seabed sediment (ρ) is given by:

$$\rho = \rho_f n + \rho_s(1-n) \tag{9}$$

in which ρ_s denotes the density of solid particles. The effects of partial saturation in sediments are captured by modifying the sediment compressibility (β) applicable for small degree of unsaturation written as:

$$\beta = \frac{1}{K_w} + \frac{1-S_r}{p_{w_0}} \tag{10}$$

where K_w, S_r and p_{w_0} represent bulk modulus, degree of saturation, and absolute water pressure, respectively.

BOUNDARY CONDITIONS

At water surface, regular linear waves are applied, and the identical dynamic pressure is implemented (as a known boundary condition) written as:

$$p_f = \frac{\rho_f g H}{2} * \cos(Kx - \omega t) \tag{11}$$

where H is wave height, $K = 2\pi/L$ wave number (L as wave length), and $\omega = 2\pi/T$ wave circular frequency (T as wave period), g gravitational acceleration, x spatial variable in horizontal direction, and t denotes time.

The length of truncated computational domain is chosen equal to a coefficient of wave length and periodic boundary conditions are implemented along lateral boundaries. Continuity of

flux and pressure (hydrodynamic pressure in fluid domain with pore fluid pressure inside the sediments) at the interface of fluid and seabed domains (S_1 in Figure 1) are satisfied. Along the interface of fluid and GSC domains (S_2 in Figure 1), normal velocity of fluid particles ($\frac{\partial \emptyset}{\partial n}$) is equal to that of geotextile. Also, the dynamic pressure is identical to normal traction of structure.

The strong interaction and perfect bond between the geotextile layer and confined soil is assumed. Therefore, the continuity of displacement and normal traction are satisfied. No flow boundary condition as well as zero displacement of soil skeleton is assumed along the rigid base of seabed with finite thickness. At the interface of GSC and seabed, a perfect bond is assumed in which no relative displacement between domains occur. Also, no flow boundary condition for pore fluid flow is implemented, and the normal component of total stress tensor of sediments is equal to the normal traction of the structure domain.

NUMERICAL RESULTS AND DISCUSSION

The above governing equations in conjunction with boundary conditions are solved using finite element method in time domain. All equations are introduced into COMSOL (COMSOL Multiphysics, version 5.3.a), and at each time step the output results of field variables ($\emptyset, u_{st}, v_{st}, u, v, p$) are obtained. A parametric study evaluating the effect of wave height on the extent of instantaneous liquefaction is carried out. The influence of soil and other wave characteristics on the response was not a part of this study.

Wave-Induced Seabed Response. The interaction problem of a single GSC mounted on horizontal seabed with finite thickness subjected to waves is studied (Figure 2), and the parameters used in analyses are tabulated in Table 1. The geotextile layer is assumed to have a 5 mm thickness with the density of $400\ Kg/m^3$ and Poisson's ratio υ=*0.4*. The cross section of GSCs used in the modeling is part of an elliptical shape (Khalilzad and Gabr 2011); however, in this study, for simplicity and to obtain the normal component of stress vector for geotextile layer, circular cross section for GSC is selected with dimensions (height and width) similar to those of GSC structure deployed near Galveston shorelines in Texas. The wave breaking threshold for progressive waves is chosen as *H/d=0.78*, and the criterion for water depth ratio of shallow water is $d/L \leq 0.05$ (Dean and Dalrymple 1984). In order to simulate a storm condition, the adopted values of wave steepness and water depth ratio are 0.75 and 0.06, respectively (the latter is slightly larger than $d/L = 0.05$). The domains are discretized by unstructured triangle mesh with various element size.

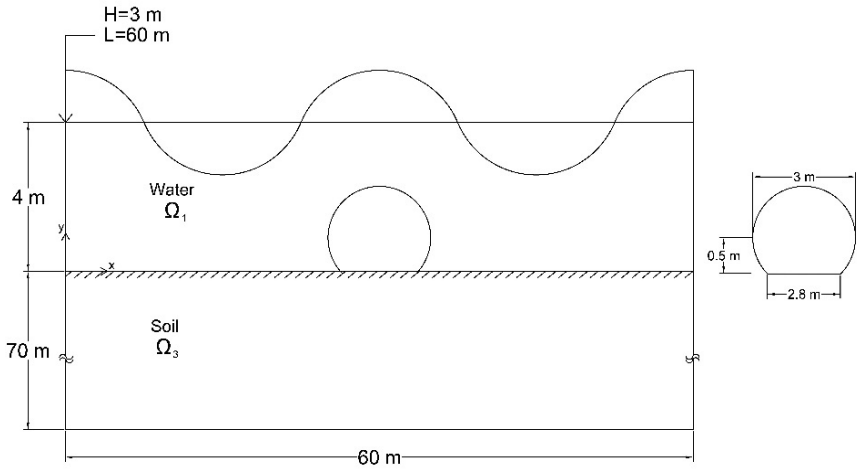

Figure 2. Model Dimensions and Wave Characteristics

Table 1

Input data

Wave Characteristics			
Wave Period (s)	10	Wave Height (m)	1.5,3
Seabed and GSC Characteristics			
Permeability (m/s)	1×10^{-4}	Porosity	0.35
Water Bulk Modulus (Pa)	2×10^{9}	Fluid Phase Density (Kg/m^3)	1000
Solid Phase Density (Kg/m^3)	2650	Poisson's Ratio	0.3
Shear Modulus of Sediment (Pa)	5×10^{7}	Shear Modulus of Sand Fill (Pa)	5×10^{7}
Shear Modulus of Geotextile (Pa)	2×10^{9}		

Following a parametric study, the highest mesh resolution with the maximum element size of 2 mm is adopted for the thin geotextile layer and maximum element size at locations away from the structure is limited to 0.3 m.

The variations of wave-induced maximum pore water pressure and shear stress within the seabed for the points located on a vertical line at x=0.5 m from right side of the structure are shown in Figure 3 (for the wave height $H = 3\ m$). Negligible shear stress and high pore water pressure magnitude at seabed surface are observed near the seabed surface.

Wave-Induced Instantaneous Liquefaction. The waves generate hydrodynamic pressure within the fluid domain. This pressure is equal to pore fluid pressure along the seabed surface. The presence of excess pore water pressure in sediments reduces the effective stress and consequently the shear strength of seabed. Under certain wave conditions, the mean effective stress may reach zero values (instantaneous liquefaction)

s

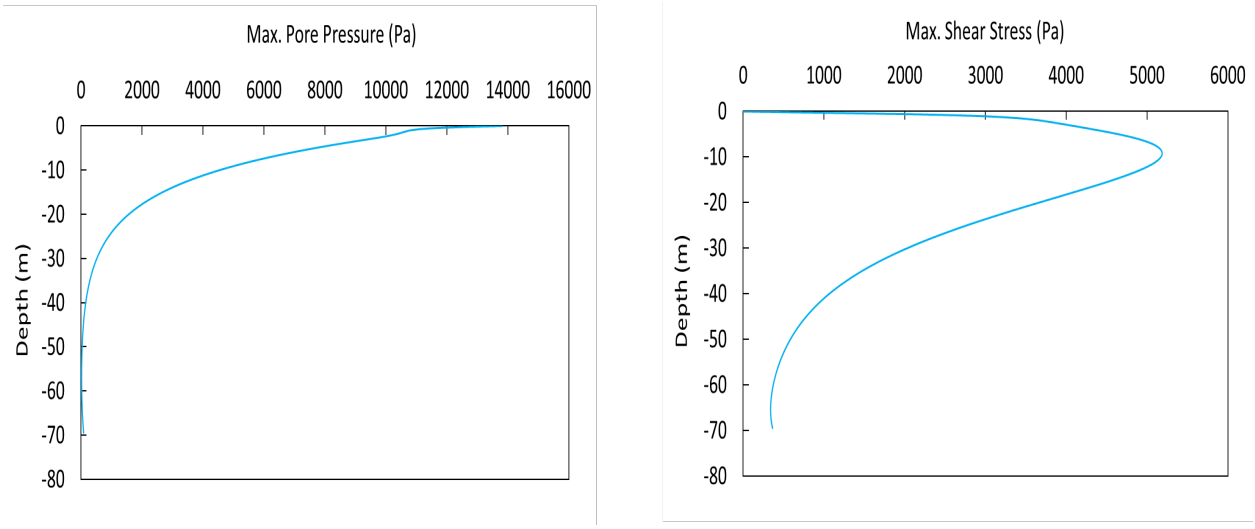

Figure 3. Distribution of pore water pressure and shear stress within seabed depth for points at 1.9 m distance from the centerline of the GSC

expressed as:

$$\sigma'_m = 0 \quad \text{or}$$

$$\bar{\sigma}'_g + \bar{\sigma}'_w = 0 \tag{12}$$

In the above equation, $\bar{\sigma}'_g$ and $\bar{\sigma}'_w$ denote mean effective stress for geostatic and wave condition, respectively. The geostatic term is obtained accounting for the submerged weight of GSC and seabed.

The extent of instantaneous liquefaction near the structure is shown in Figure 4 for two wave heights $H = 3\ m$ and $H = 1.5\ m$ at the same time t=T assuming that sediments are partly saturated with a uniform degree of saturation $Sr = 0.98$ within the seabed. The presence of gaseous sediments within the seabed is not uncommon [OKUSA 1985]. The slight unsaturation of the seabed is mostly due to gas bubbles occluded in the pore water. However, partly-saturated sediments are expected to be near the bed surface as the pressure at larger depth will force the air into the pore water and increases the saturation level. The dimensions of liquefied zones are scaled with respect to dimensions of the GSC. As shown in Figure 4, instantaneous liquefaction occurs below the wave trough since in those locations an upward seepage force is developed in the seabed resisting the downward gravitational forces (at each time step instantaneous liquefaction occurs

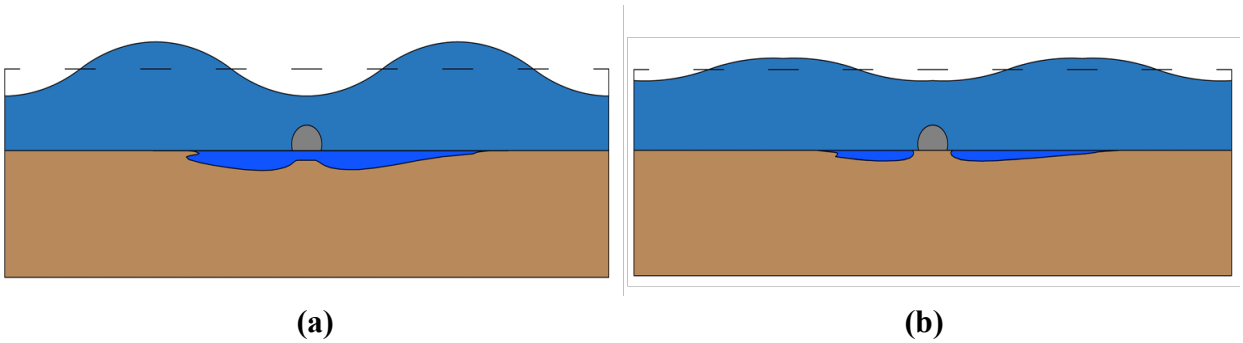

(a) (b)

Figure 4. Extent of wave-induced I liquefaction (dark blue) near the GSC at t = T for different wave heights: a) H=3 m, b) H=1.5 m

in the seabed depending on the wave profile, and in Figure 4 it is shown for t=T). Stronger waves induce greater stresses inside the sediments resulting in larger liquefied zones. The weight of structure suppresses liquefaction to some extent and, as shown, as the maximum liquefication depth occurs at locations away from the structure. The sediments within the liquefied zones may lose their shear strength resulting in sediment transport and scour around the structure. In such condition, and due to reduction of soil confinement, bearing capacity issues of the foundation soil are probable leading to sinking of the GSC into the seabed and differential settlements (depending on the location of liquefaction zones). Similar scenario occurred during Hurricane Ike as shown in the earlier study by Khalilzad and Gabr (2011).

It is worth mentioning that no instantaneous liquefaction within seabed has been observed for fully saturated sediments. Such observation is consistent with analytical solutions (Ulker et al. 2009). The gradient of wave-induced pore water pressure within the gas-laden sediment near the seabed surface is higher than that for the saturated sediment. Thus, the upward seepage force resulting in instantaneous liquefaction may be larger for partly-saturated sediment. Other form of liquefaction due to progressive buildup of pore water pressure (progressive liquefaction) has been observed in loose to medium-dense non-cohesive fully saturated sediments (Rahman 1991).

Wave Loading on GSC. The distribution of wave loading acting on GSC for different times are illustrated in Figure 5. The loading values are related to the position of wave profile. At t=T and t=T/2, right above the centerline of GSC wave crest and wave trough are occurring, respectively leading to positive and negative values of dynamic pressure, correspondingly, with symmetric distributions. Similarly, at t=T/4 and t=3T/4 wave crest generates at the surface on the right and left side of the structure, respectively. In these time steps, non-symmetric loading distribution induced by the wave is acting on the structure. The non-symmetric loading distribution may lead to differential settlement of the GSC, with an impact on the stability of the GSC-structures, especially if these were constructed in stacked configuration.

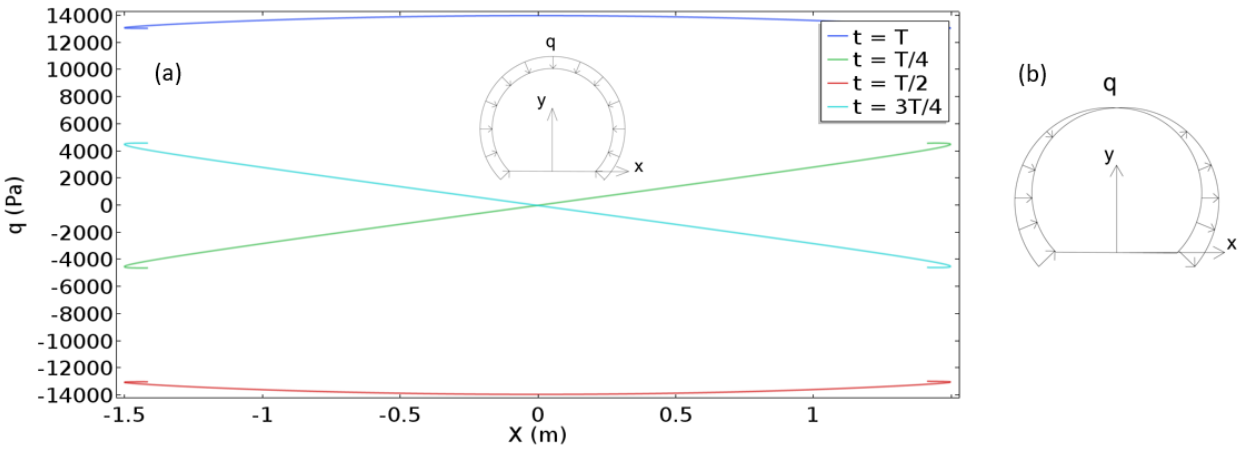

Figure 5. Distribution of Wave Loading on the GSC: a) for different times (t=T/4, T/2, t=3T/4, t=T), b) free body diagram at t=3T/4

CONCLUSION

In this study, response and instability of foundation soil around the GSC under progressive surface waves are analyzed. The distribution of loading on the structure under wave action is also obtained. The related governing equation and boundary conditions are programmed into a numerical model in COMSOL, for coupled analyses of the wave, geotextile container, and seabed domains. The following conclusions are obtained based on the results presented herein:

1. In shallow water, the pore water pressure within the seabed sediments caused by waves is significant and results in instantaneous liquefaction around the GSC. Such liquefaction can lead to scour and loss of soil confinement around the structure.
2. Even for smaller wave heights, instantaneous liquefaction appears to be probable. However, the weight of the structure suppresses such liquefaction to some extent.

It is noted that the values and distribution of wave loading on the GSC is a function of wave profile. At a certain time with respect to non-symmetrical loading distribution, differential settlement can occur given the difference in loading magnitude along the structure cross section. Such deformation can lead to affect the serviceability and instability of the geotextile sand container-structures.

AKNOWLEDGMENT

This study is supported by a grant from Coastal Study Institute of North Carolina (CSI) and North Carolina State University.

REFERENCES

Bathe, Klause (1996). "Finite Element Procedure." *Prentice Hall Inc*.

Biot M.A. (1956). "The theory of propagation of elastic waves in a fluid-saturated porous solid. I. Low-frequency range." *J. Acous. Soc. Am.,* 28, 168–178.

COMSOL Multiphysics® v. 5.2. www.comsol.com. COMSOL AB, Stockholm, Sweden.

Dean, R., Dalrymple, R. (1984). "Water Wave Mechanics for Engineers and Scientists." *World Scientific Publishing Co.Pte.Ltd*, p. 170.

Heilman, D.; Perry, M.; Thomas, R.; and Kraus, N. (2008). Interaction of Shore-Parallel Geotextile Tubes and Beaches along the upper Texas Coast, Vicksburg, MS: U.S. Army Corps of Engineers, Technical Note ERDC/CHL CHETN-II-51 (January), 18p.

Khalilzad M., Gabr M.A. (2011). External Stability of Geotubes Subjected to Wave Loading, Journal of Geotechnical Risk Assessment and Management, GSP 224.

Kraus, N. C. and Lin L. (2009). Hurricane Ike along the upper Texas Coast: An Introduction *Shore & Beach*, Vol. 77, No. 2, 1-8

Mirafi (2004), Physical Properties of Geosynthetics, Technical Brochure.

Neves L.P. (2011), Experimental Stability Analysis of Geotextile Encapsulated-Sand Systems under Wave-Loading, PhD Dissertation, University of Porto.

Okusa S., (1985), Wave induced Stress in Unsaturated Submarine Sediment, Geotechnique 35(4), 517-532.

Rahman, M.S. (1991), Wave-Induced Instability of Seabed: Mechanism and Conditions. Marine Geotechnology 10(4), 277–299.

Recio, J. (2008). Hydraulic Stability of Geotextile Sand Containers for Coastal Structures, PhD Dissertation, Braunschweig University of Technology.

Robertson, N., Riggs, H., Solomon, Yim, and Young, Yin (2007). Lessons from Hurricane Katrina Storm Surge on Bridges and Buildings, *Journal of Waterways, Port, Coastal and Ocean Engineering*, ASCE 0733-950X, 133:6, 463.

Ulker, M. B. C., Rahman, M.S., Jeng, D.S. (2009), Wave-induced Response of Seabed: Different Formulations and Their Applicability, Applied Ocean Research. 31, 12-24.